REPORT DOCUMENTATION PAGE

Form Approved
OMB No. 0704-0188

1. REPORT DATE *(DD-MM-YYYY)*	2. REPORT TYPE	3. DATES COVERED *(From - To)*
12/19/2019	Final Technical Report	06/01/2015 to 04/30/2019

4. TITLE AND SUBTITLE
High Reynolds Number Stratified Turbulent Wakes: Internal Wave Energetics, Self-similarity and Subgrid-scale Modeling

5a. CONTRACT NUMBER
N00014-15-1-2513

5b. GRANT NUMBER

5c. PROGRAM ELEMENT NUMBER

6. AUTHOR(S)
Diamessis, Peter J.

5d. PROJECT NUMBER

5e. TASK NUMBER

5f. WORK UNIT NUMBER

7. PERFORMING ORGANIZATION NAME(S) AND ADDRESS(ES)
School of Civil and Environmental Engineering
220 Hollister Hall
Cornell University
Ithaca, NY 14853

8. PERFORMING ORGANIZATION REPORT NUMBER

9. SPONSORING/MONITORING AGENCY NAME(S) AND ADDRESS(ES)
Office of Naval Research
875 North Randolph Street
Arlington, VA 22203-1995

10. SPONSOR/MONITOR'S ACRONYM(S)
O.N.R.

11. SPONSOR/MONITOR'S REPORT NUMBER(S)

12. DISTRIBUTION/AVAILABILITY STATEMENT
Approved for public release; distribution is unlimited.

13. SUPPLEMENTARY NOTES

14. ABSTRACT
The work funded by this grant is founded on unique stratified turbulent sphere wake database generated by massively parallel Large Eddy Simulations spanning a range of values of body-based Reynolds, Re, and Froude, Fr, numbers. The flow phenomenology observed with increasing Re indicates that a novel form of persistent, highly-layered, and space-filling turbulence emerges in the late-wake core. In addition to quantifying and parameterizing the characteristics of this layered turbulence, the energetic content, directional preference and along-wake-periphery of wake-radiate internal waves has been systematically studied. Internal waves become a dominant contributor to the wake energy budget, particularly at high Re.

15. SUBJECT TERMS
Stratified turbulent wakes, high Reynolds numbers, turbulence in the strongly stratified regime, internal waves, high-order element-based numerical methods, high-performance computing.

16. SECURITY CLASSIFICATION OF:			17. LIMITATION OF ABSTRACT	18. NUMBER OF PAGES	19a. NAME OF RESPONSIBLE PERSON
a. REPORT	b. ABSTRACT	c. THIS PAGE			Peter J. Diamessis
					19b. TELEPHONE NUMBER *(Include area code)*
U	U	U	SAR	12	607-255-1719

FINAL REPORT, December 18, 2019

Contract Information

Contract Number	N00014-15-1-2513
Title of Research	High Reynolds Number Stratified Turbulent Wakes: Internal Wave Energetics, Self-similarity and Subgrid-scale Modeling
Principal Investigator	P. J. Diamessis
Organization	School of Civil and Environmental Engineering, Cornell University
Contracting Officer	Dr. Peter Chang

Technical Section

Technical Objectives

The research supported by ONR grant number N00014-15-1-2513 focused on the following primary technical objectives:

- Examine the flow structure and large-scale turbulent characteristics (length/velocity scales and non-dim. params.) of sphere wake turbulence in the strongly stratified regime as a function of *Re* and *Fr*.
- Predict accessibility and duration of the strongly stratified regime for a wake at a given pair of sphere-based Reynolds, *Re,* and Froude, *Fr*, numbers.
- Quantify the temporal evolution of wake power radiated into internal waves, with a particular focus on contrasting the strongly stratified intermediate-to-late wake's contribution to this phenomenon with respect to the early wake.
- Determine directional preference and along-wake-periphery distribution of radiated internal waves.

A parallel, method-focused, primary objective has consisted of initiating an upgrade of the temporal, body-exclusive, wake-flow solver, originally built by the way, in terms of improved numerical methods and parallel performance.

Results

The results obtained in pursuit of the above objectives may be grouped in the following categories, to each of which we dedicate its own section. Central to our work is the development of a unique implicit Large Eddy Simulation (ILES) dataset of stratified turbulent wakes, spanning three $Re = UD/\nu = \{ 5\times10^3 , 10^5 , 4\times10^5 \}$ and three $Fr = 2U/(ND) = \{4, 16, 64\}$. The value of $Re = 4\times10^5$ is the highest yet reported in the literature, offering the deepest probe so far into the strongly stratified regime, as elaborated below. These state-of-the-art simulations were enabled by a DoD Frontier Award. Typical resolutions at $Re = 4\times10^5$ have consisted of $1024 \times 512 \times 1105$.

(i) Wake turbulence in the strongly stratified regime

In this section, we summarize the key findings of our work, documented in full detail in the paper by *Zhou and Diamessis* (2019). The original objective of this effort was to identify potential *Re* scalings of turbulent flow characteristics. We have been successful in meeting this objective, while we have also identified a potentially new regime of wake turbulence at sufficiently high *Re* in the intermediate-to-late-wake: that of the strongly stratified regime, where buoyancy is the $O(1)$ controlling mechanism of wake flow physics, yet patchy (and potentially space-filling) turbulence develops in high-aspect ratio layers, which have significant horizontal extent and are highly focused in the vertical.

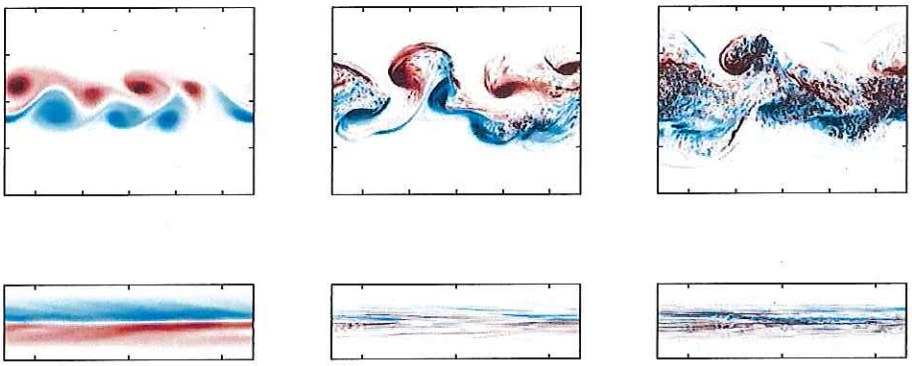

Figure 1: Colormaps of (a)–(c) vertical vorticity ω_z (x,y) fields at $Nt = 120$ sampled at the Oxy horizontal midplane ($z = 0$) for $Fr = 4$, simulations at $Re = 5 \times 10^3$, 10^5 and 4×10^5, respectively (from left to right) in top three panels. Bottom three panels show spanwise vorticity ω_y (x,z) fields for the same instances sampled at the Oxz vertical midplane ($y = 0$). The sphere travels from left to right. The length of the visualization window is, in the top panels, 80/3 D in x and 20D and, in the bottom panels, 40/3 D in x and 4D in z. The colorbar limits are adapted to highlight the key structural features of the vorticity fields.

The structural imprint of wake turbulence in the strongly stratified regime, for wakes at $Fr = 4$, is shown in Figure 1, at a non-trivially late time $Nt = 120$. Laboratory-scale $Re = 5\times10^3$ simulations indicate the presence of diffuse "pancake"-like quasi-horizontal eddies in the centerline stream-span plane accompanied by inclined diffuse shear layers in the centerline stream-depth plane. As identified by previously ONR-funded research, at a much higher value of $Re = 10^5$, embedded within the late-wake pancakes are intermittently positioned patches of finer-structure motion linked to Kelvin-Helhmoltz-like instabilities driven by the spontaneous vertical shear induced by buoyancy. The high *Re* dataset shows that the resultant secondary turbulence motions are far more-space filling at late times, since the turbulence supports an even greater dynamic range as suggested by values of the activity parameter, *Gn*, of $O(30)$, a measure of the scale separation between largest overturning scales and the turbulence Kolmogorov scale, or higher at these later times. Observations at other, higher, *Fr*, are consistent with those of Figure 1. As computational power grows, one is expected to reach even higher sphere-based *Re*, and values of $Gn \approx O(100)$ in the intermediate-to-late wake, where this intermittent highly layered turbulence is likely to occupy the entire wake cross-section.

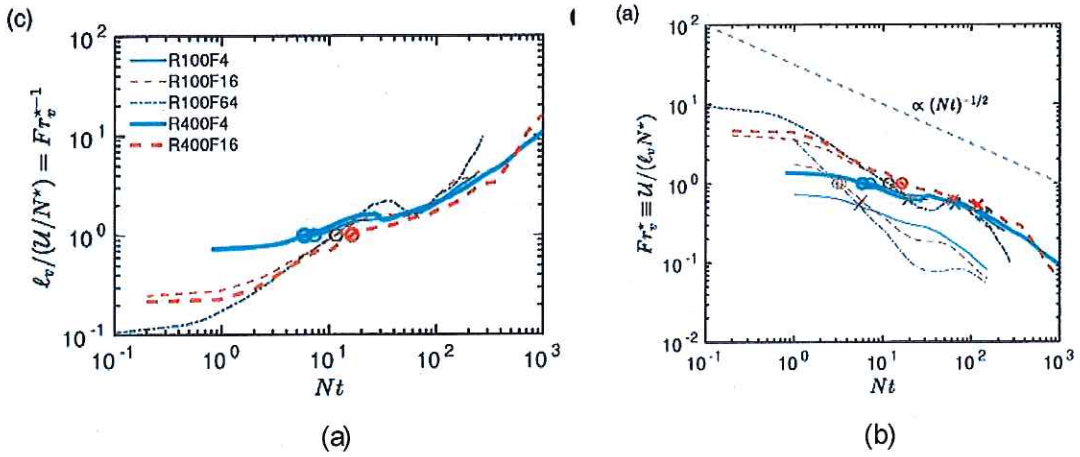

Figure 2: (a) Inverse cyclical vertical Froude number $Fr_v^{*-1} \equiv l_v / (U/N^*)$ as a function of time. (b) Actual cyclical vertical Froude number Fr_v^* timeseries. Results are limited to the higher *Re* considered, as low *Re* data are incapable of supporting overturning turbulence in the strongly stratified regime. The circles in (a) mark the unity crossing time of Fr_v^*. The crosses in (b) mark the unity crossing time of buoyancy Reynolds number $\mathfrak{R}$ (see Figure 3b). In (a), the lightly shaded region corresponds to $1 < Fr_v^{*-1} < 2$, a characteristic dynamical signature of the strongly stratified regime.

As first step towards quantitative analysis, the horizontal and vertical integral scales of the wake turbulence has been computed by integrating, in wavenumber space, 1-D spectra of turbulent kinetic energy in the streamwise and vertical direction. The resulting length scales, along with the characteristic r.m.s.-averaged value of fluctuating horizontal velocity U within the wake core, may then be used to compute *local turbulent integral-scale-based* non-dimensional parameters of the flow inside the wake, thereby providing perspective into its dynamical state. Figure 2a shows the timeseries of the vertical integral scale as normalized by U and the *cyclical* buoyancy frequency (in *Hz*) N^*, for all Fr at the two higher Re considered. All curves appears to collapse in the interval $10 \leq Nt \leq 100$. If one inverts the quantity shown in the vertical axis, a *local* (in a temporal sense) vertical Froude number, Fr_v emerges (Figure 2b) What is most interesting is the near-constant $Fr_v \approx O(1)$ which appears in the window $10 \leq Nt \leq 40$, followed by a slow decay of this value, particularly in the $Re = 4\times10^5$ data: over focused vertical layers of height l_v, the turbulence can consistently overturn against the stratification at times where buoyancy is the primary controlling mechanism of flow dynamics. $Fr_v \approx O(1)$, with Fr_h is a characteristic feature of turbulence operating in the strongly stratified regime.

That buoyancy is the dominant controller of flow evolution is confirmed by Figure 3a, which shows timeseries of the *local horizontal Froude number, Fr_h*. As buoyancy rapidly controls the turbulence integral scale in the horizontal, eventually controlling the rotation of quasi-horizontal pancake vortices, it has dropped to values of approximately 0.03 by the time $Fr_v \approx O(1)$ is established. Note that the equivalent *local horizontal Reynolds number, Re_h*, may be used with Fr_h to form the parameter $\mathfrak{R} = Re_h\, Fr_h^{\,2}$, regarded by some as a *buoyancy Reynolds number*. $\mathfrak{R}$ is a measure of the ability of the flow in the strongly stratified regime to support Kelvin-Helmholtz-like instabilities. At values greater than $O(10)$ it also tracks Gn and offers an alternative measure of the dynamic range of the turbulence. Re_h and $1/Fr_h$ may be combined together to provide a regime diagram, where one may monitor the development of stratified turbulent wake as a transitions through different flow regimes. The key take-home message is that for sufficiently high body based Re, after having transitioned through classical

Kolmogorov-like active turbulence and weakly-stratified turbulence (Fr_h slightly smaller than unity), the flow will reside, for some time in the strongly stratified regime, as represented by the top right triangle in the diagram. The higher Re, the longer this residence time and the more complex the physics of this strongly stratified flow, a large aspect of which remains unexplored and pushes the limits of currently computational resources. The ultimate objective would be to study a flow at very low Fr_h , yet $\mathfrak{R} \approx 100$, as any operational wake will transition through such a state. In other words, one wants to push inside the triangle as far to the right as possible. The existing ILES have indicated that we are only at the cusp of such a regime, where for key turbulence characteristics, will ultimately be Re –independent.

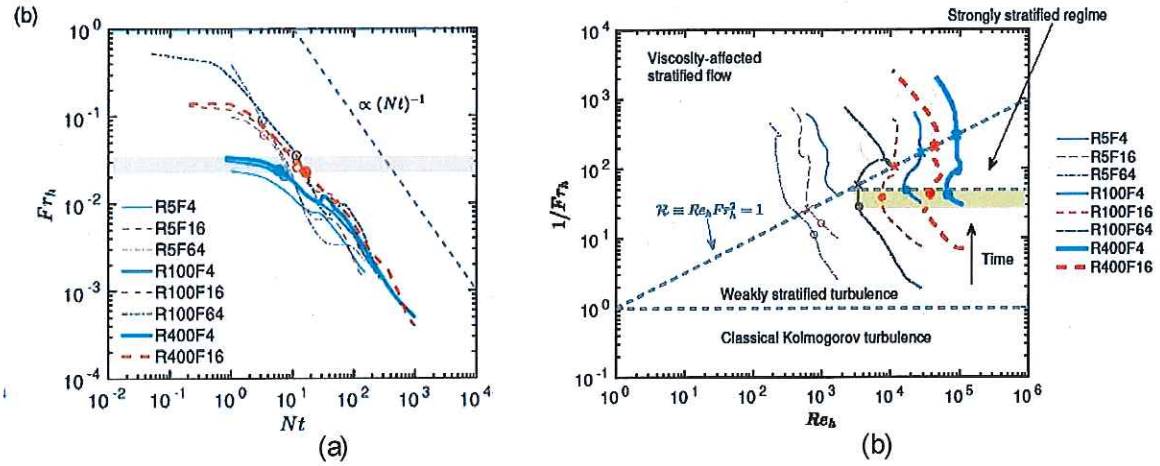

Figure 3: (a) Variation of horizontal turbulent Froude number Fr_h with the dimensionless time Nt. The shaded region is (b) corresponds to $0.021 < Fr_h < 0.035$, the range of Fr_h values at which the wakes enter the strongly stratified regime. (b) Regime diagrams of stably stratified turbulent wakes examined in this project. Shaded regions and symbols used here are the same with those considered in Figures 2 and 3a.

Through a straightforward scaling exercise, by exploiting our ILES database, one may attempt to then identify the dependence of $Re_h^{\downarrow}$, the horizontal local turbulent Reynolds number, on Re and Fr. As shown in Figure 4, we find that $Re_h^{\downarrow} \sim Re\ Fr^{-2/3}$. Moreover, $Re_h^{\downarrow} \geq 2{,}500$ appears to guarantee that the wake will enter the stably stratified regime. Finally, the duration of the stably stratified regime has been found to scale with $Re^{1/2}\ Fr^{-1/3}$. The operational implications of the above scalings are several.

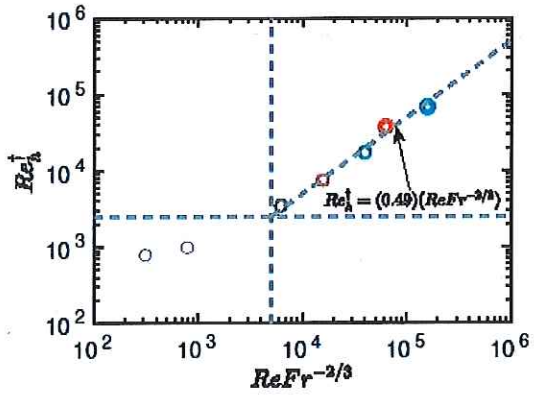

Figure 4: Transitional horizontal turbulent Reynolds number Re_h † h as the flow enters the strongly stratified regime and its dependence on the wake's body-based parameters Re and Fr. The horizontal line corresponds to the lower bound of Re_h † in order for the wake to access the strongly stratified regime. The vertical line corresponds to the threshold value of $Re\ Fr^{-2/3}$ for wakes accessing the strongly stratified regime.

(ii) Energetics and Directionality of Internal Wave Radiation

Internal wave radiation by a stratified wake has been characterized, for all Re and Fr considered, by computing the energy flux vector, $p'\vec{u}$, through the entire surface of wake-following elliptical cylinder. The elliptic cylinder's limits are defined as the locations where the total kinetic energy (KE ; no Reynolds decomposition is performed in this study) reaches 0.5% of its peak value. Examples of the wake-following elliptic cylinder, throughout the evolution of a particular wake simulation, are shown in Figure 5. The elliptic cylinder tightly bounds the wake and adjusts as the wake, constrained in the vertical by stratification, expands in the horizontal. Furthermore, the elliptic cylinder resides immediately outside the wake, such at its exterior, extending into the ambient fluid, the flow field is dominated strictly by internal waves as evidenced by zero values of potential vorticity (an indicator of turbulence, yet not internal waves ; *Watanabe et al.* 2016) in this region. Immediately outside of the elliptic cylinder, the flow physics is most likely to be dominated by nonlinear wave-wave interactions. An example of contours of the magnitude of $p'\vec{u}$ on the surface of the wake-following-elliptic cylinder is shown in Figure 6.

The power released by the wake into internal waves is found by computing the integral of the energy flux vector,:

$$P_W = \int \oint p'\vec{u}\hat{n}dsdx$$

where the surface integral is calculated over the area of the elliptic cylinder and the outer 1-D integral is computed across the full length of the computational domain. Since the ellipse is an intrinsically periodic domain, through the interpolation onto Fourier collocation points uniformly positioned along the periphery of the ellipse, one can compute the above integral with spectral accuracy.

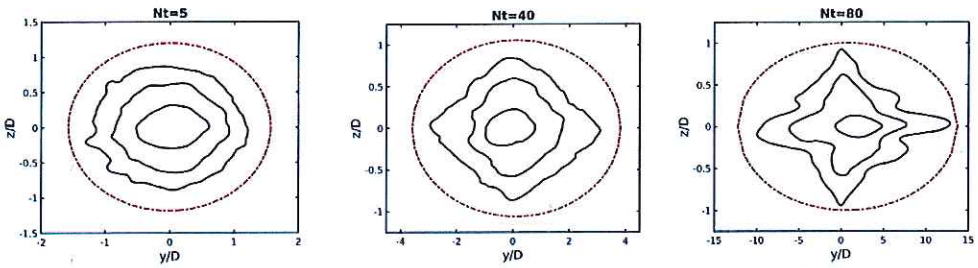

Figure 5: Cross-sections of the streamwise-mean kinetic energy for $Re = 10^5$, $Fr = 4$. Solid (black) contours correspond to values of 0:5%, 5%, and 50% of the maximum value at each time. The dashed (red) contour shows the fit of the elliptic cylinder used for the wave flux calculation.

Timeseries of the appropriately normalized wake-radiated internal wave power, as defined above, are shown in Figure 7 for all values of *Re* and *Fr*. The first noteworthy observation is that, for a given *Fr*, the peak wave power is the same across all *Re*. The first burst of internal wave radiation, associated with the transition of the wake from actively three-dimensional turbulence dynamics to the onset of buoyancy control, is apparently controlled by the larger-scales of the flow in the wake core which are *Re*-independent. Additionally, the peak power released into internal waves decreases with increasing *Fr*. Nevertheless, a distinct difference is observed as one examines the timeseries at later times: high *Re* wakes emit a non-trivial amount of energy into internal waves.

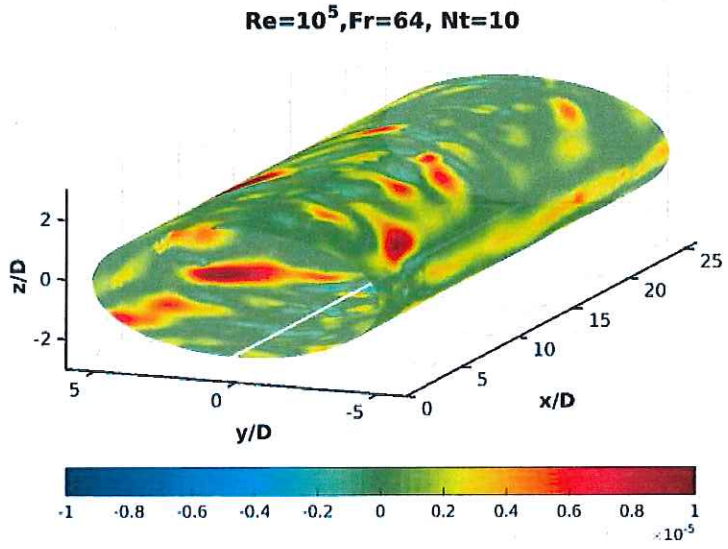

Figure 6: Example of wake following elliptic cylinder at earlier times for the $Re = 10^5$, $Fr = 64$ case. Shown are contours of the magnitude of wave energy flux vector $p'\vec{u}$.

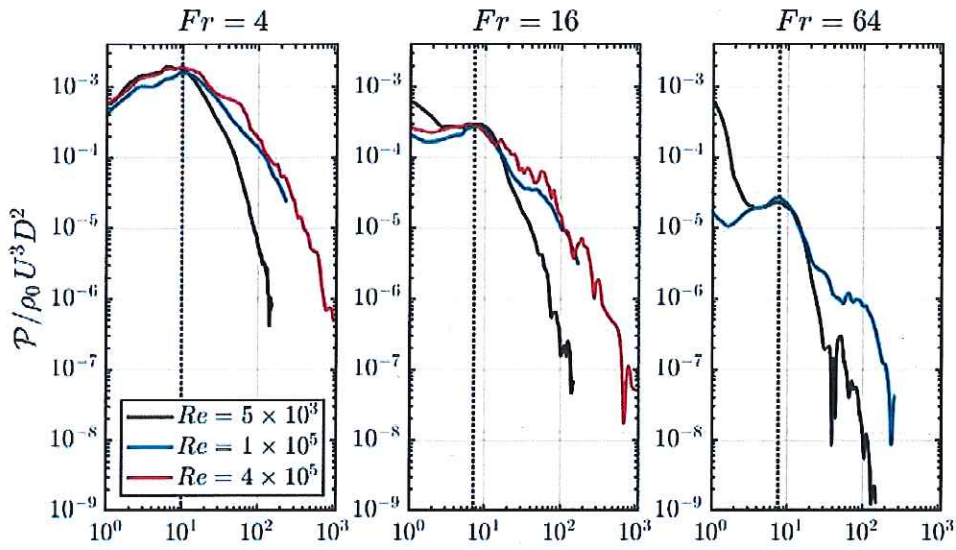

Figure 7: The instantaneous wave power radiated through a wake-following elliptic cylinder, scaled using the sphere diameter and tow speed, *U* and *D*, respectively.

Assuming that the rate of change of kinetic energy *per unit volume* in the wake scales as U_0^3/L_H, where U_0 and L_H, are the maximum mean wake centerline velocity and mean wake width, one may use standard *Fr*-scalings for these two mean quantities, to deduce that the wake power should scale with $Fr^{-7/3}$. Figure 8 confirms the efficacy of this scaling, as restricted to collapsing the associated timeseries for all *Re* and *Fr* at the time of peak internal wave power emission. The $Fr^{-7/3}$ scaling carries significant predictive utility.

The time-integrated values of internal wave power, a measure of the total energy released into internal waves at any given time by the wake, are shown in Figure 9. The left panel shows the total internal wave energy, as sampled over a horizontal plane, whose offset from the wake edge is a function of *Fr*. The right panel shows the same quantity, computed over the entire wake-following elliptic cylinder. A higher amount of internal wave energy is recorded in the elliptic cylinder case, as the horizontal plane cannot capture waves propagating closer to the horizontal. Consistent with what is shown in Figure 8, one sees that an increase in *Re* produces a slow increase in total energy released into internal waves at any given *Fr*. This total energy is reduced, as *Fr* increased. Interestingly, at $Fr = 64$, one notices no gain in radiated internal wave energy as *Re* increased. Potentially, there is a critical *Fr* value above which internal wave energy radiation is highly inefficient.

Figure 10 shows the space-time contours of streamwise-averaged wave power flux or intensity normal to the surface of a wake-following elliptic cylinder for the Fr=4 datasets. The particular quantity allows one to determine where along the wake periphery there is a preference for internal wave radiation. Whereas at early times, there is a preference for the left/right edges of the wake, regardless of *Re*, as one moves forward in time in the high *Re* cases, it is visible that strong radiation from the wake edges is accompanied by bursts of IW activity which are more randomly distributed along the wake periphery. Results for the two higher *Fr* datasets are consistent with what is shown in Figure 11.

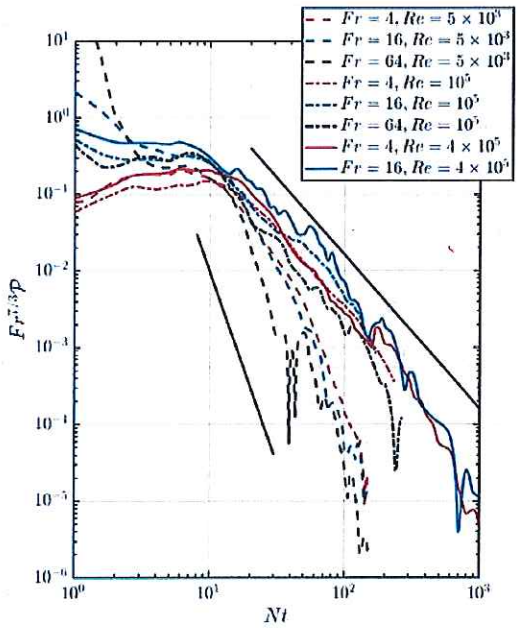

Figure 8: Scaled wave power time series from elliptic cylinder analysis. The upper and lower solid lines have a slope of -2 and -5 respectively. The wave power is scaled by the volume of the elliptic cylinder.

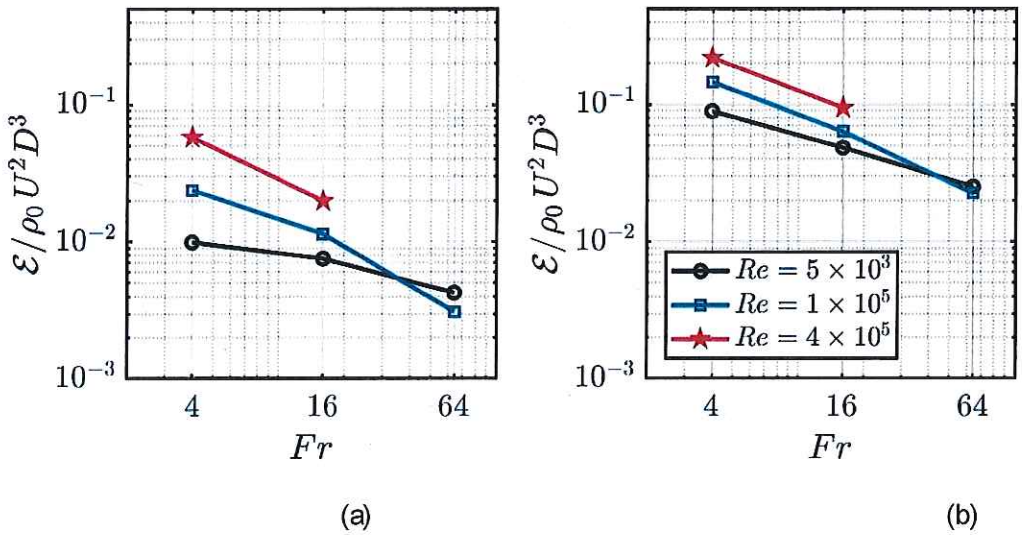

Figure 9: The Froude number dependence of the total wave energy, integrated over time and area of the corresponding reference surface, radiated through a fixed horizontal plane (a) and a wake-following elliptic cylinder (b) over the course of each numerical experiment for all 3 *Re* values considered in this study.

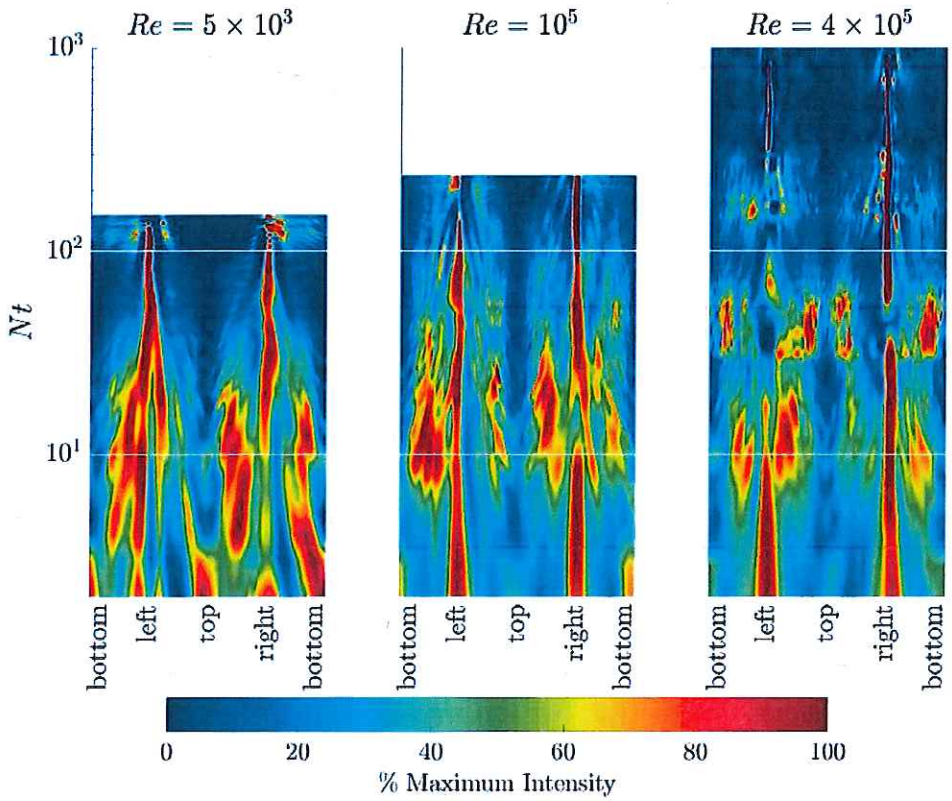

Figure 10: Space-time contours of internal wave intensity normal to a wake-following elliptic cylinder, scaled at each time as a percent of the instantaneous maximum, for the $Fr = 4$ simulations. Horizontal axes display the tangential coordinate around the cylinder cross-section. The horizontal white lines mark times $Nt = 10$ and 100.

The angle between the power flux vector and the horizontal can be used to quantify the direction of radiation (not necessarily propagation; see the discussion below) of the internal waves emitted from the wake. Using the wave power flux vector field sampled throughout the entire the elliptic cylinder at each instant in time, the joint probability distribution of the magnitude and horizontal propagation angle can be constructed. Subsequently the mean power flux can be calculated as a function of the horizontal propagation angle as shown in the radial histograms of Figure 11, which focuses on the $Fr = 4$ datasets. At $Fr = 4$, one sees a relatively broadband signal appear at very early times. In the interval $10 \leq Nt \leq 20$ internal waves tend to be radiated at angles in the [20°,60°] interval . At $Re = 5 \times 10^3$, any internal waves radiated by the wake are emitted at a near-horizontal angle. This is not the case for the two highest Re, where waves radiated within the angle interval [15°,45°] with waves emitted at angles greater than 15° occurring at times $Nt = 30$ and 45 at $Re = 10^5$ and 4×10^5 , respectively. These intermediate-to-late time waves are clearly associated with turbulence in the strongly stratified regime and, are as such, generated by a completely different flow structure than their earlier time counterparts. The corresponding radial histograms for $Fr = 16$ and 64 (not shown here) reveal similar trends. A potentially noteworthy feature of the $Fr = 64$ dataset is the occurrence of waves radiated at near-vertical angles, i.e., with frequencies very close to those of the buoyancy frequency. We defer interpretation of these vertically propagating waves to future work.

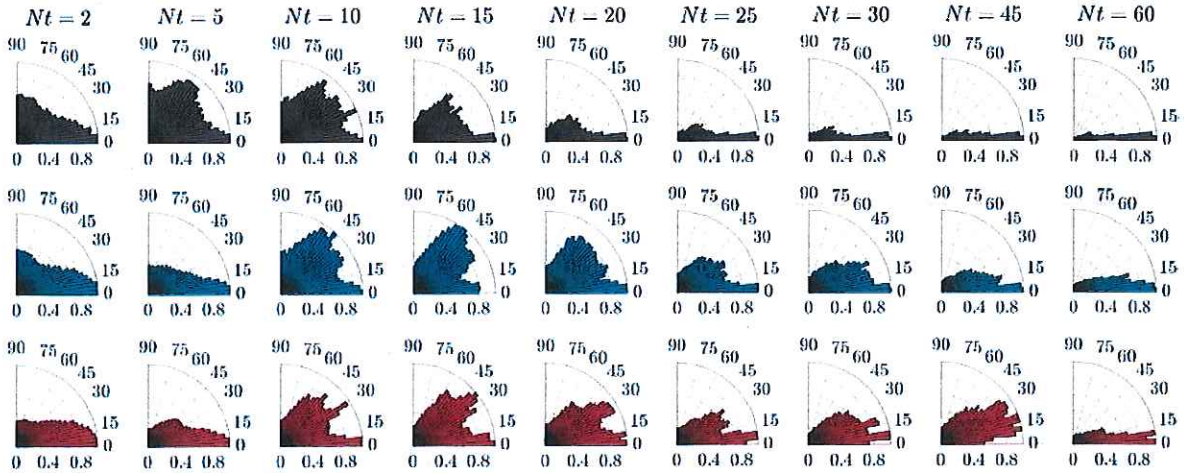

Figure 11: Mean power flux dependence on the radiation angle relative to the horizontal for the $Fr = 4$ experiments at $Re = 5 \times 10^3$ (upper), $Re = 10^5$ (middle), and $Re = 4 \times 10^5$ (lower). The radial axis quantifies the power flux normalized by the maximum value. The azimuthal axis quantifies the wave propagation angle relative to the horizontal.

Finally, a key outstanding question is the role of internal wave radiation in the wake energy budget. To this end. Table 1 shows the wake energy lost to internal waves as normalized by the corresponding value of change in wake kinetic energy during different sub-windows of the Non-Equilibrium (NEQ) of wake evolution, when the horizontal mean/turbulent velocities inside the wake decay at a much slower rate as contrasted to their actively turbulent counterparts. It is immediately apparent that, at $Fr = 4$, at the two higher Re, internal wave radiation plays a dominant role in the wake energy budget when buoyancy has assume full control of the wake flow. At $Fr = 16$, internal wave radiation retains an important role in the wake energy budget. A similar statement may be made for the $Fr = 64$ wake, at least during intermediate times. These findings suggest that one should account for energy leakage into internal waves in more operational fast-turnaround models, a phenomenon which is currently overlooked.

Fr	Re	Early NEQ	Mid NEQ	Late NEQ	Entire NEQ
4	5×10^3	11.1%	12.1%	0.6%	11.0%
-	10^5	17.9%	52.5%	32.6%	36.2%
-	4×10^5	21.0%	74.5%	38.3%	45.6%
16	5×10^3	3.8%	9.0%	0.3%	4.9%
-	10^5	6.7%	36.3%	30.3%	13.9%
-	4×10^5	7.9%	47.2%	28.7%	19.0%
64	5×10^3	1.9%	5.7%	0.1%	2.2%
-	10^5	2.8%	22.8%	11.0%	4.5%

Table 1: The percent decrease in total kinetic energy due to internal wave radiation during the early, $2 \leq Nt \leq 10$; mid, $10 \leq Nt \leq 100$; late, $Nt > 100$; and entire Non-Equilibrium (NEQ) regime in wake evolution. Note: the last column is not equal to the sum of the previous three columns.

(iii) Modernization of High-Resolution/Accuracy Wake Flow Solver

Up until the generation of the dataset analyzed as part of this project, the PI's research group relied heavily on a Spectral-Multidomain-Penalty-Method (SMPM) solver of the incompressible Navier-Stokes equations as the primary tool for simulating wake flows. Despite the significant advances gained in physical understanding enabled by this tool, built by the PI himself 15 years ago, there was consensus within the group that the flow solver had to be improved from several standpoints which included a more robust numerical method, improved memory footprint and optimal performance on state-of-the-art DoD High-Performance-Computing systems. To this end, the final months of this project were dedicated towards updating the existing flow solver by replacing the SMPM discretization in the vertical with modal Spectral Elements. Beyond being less sensitive to numerical instability in under-resolved simulations and less prone to the formation of spurious divergence at subdomain interfaces, thereby enabling access to even higher *Re* than those reported here, the modal Spectral Element Method also is accessible to fast numerical linear algebra, by allowing the use of tridiagonal matrices in place of the large-bandwidth ones typical of higher-order element-based techniques. Assembly of all components of the flow solver, in terms of the associated operator splitting, and performance optimization is expected to have taken place in early Spring 2020.

(iv) Other Activities

In the early stages of this project, significant time was dedicated to the submission to the Journal of Fluid Mechanics, followed by two rounds of revisions, of the paper by *Zhou and Diamessis* (2016). The PI has maintained a regular collaboration with Profs. Steve de Bruyn Kops (U. Mass., Amherst) and Jim Riley (U. Washington), sustained by weekly video Teleconferences. Our ILES was used to provide initial conditions for massive high-resolution Direct Numerical Simulations of high *Re* stratified turbulent wakes, culminating in the paper by *Watanabe et al.* (2016). Additionally, this collaboration generated the DoD-HPC Hero award described below. The regular discussions with Profs. de Bruyn Kop and Rile remain ongoing.

Note that a non-trivial amount of time was dedicated by PhD student Qi Zhou, combined with discussions with Dr. Patrice Meunier at IRPHE, Marseille, France, on exploring ways to build improved self-similarity models for prediction of mean flow wake properties which account for turbulence in the strongly stratified regime. Preliminary results on this front are documented in the PhD thesis of Zhou. Efforts towards identifying parameterizations, however, remained inconclusive and will be picked up again in the future. In terms of subgrid scale model tests and developments, any efforts have been deferred to the future: this is a non-trivially complex task. Parallel work by collaborator de Bruyn Kops has identified potential avenues of physically robust SGS modeling for strongly stratified homogeneous turbulence, which, however, require significant modifications to be applied to wakes.

Ongoing/Future Work

Current work is focusing on putting closure on the re-development and performance optimization of the updated flow solver, with conclusion expected for early Spring 2020. We will then transition in regenerating our current *Re* and *Fr* dataset over domains of triple the length to ensure even more robust statistics: due to the fast code, this should be a non-time-consuming effort. At that point, we will conduct stratified wake runs at $Re = 2 \times 10^6$ and the standard range of *Fr*. Beyond investigating the physics of turbulence in the strongly stratified regime, and the associated internal wave radiation, we are aiming to

determine whether we have attained a *Re* sufficiently high to allow us to determine whether mean and turbulent statistics are *Re*-independent, at least for some fraction of wake evolution where turbulent dynamic range is sufficiently broad. In parallel, the runs will be conducted with a temporally-expanding elliptically-distributed array of virtual point probes which will allow us to correlate frequency and wavenumber content of radiated internal waves. Finally, in collaboration with computational scientist collaborator, Greg Thomsen, we will work on developing machine-learning-based tools for identification and tracking of 3-D internal wave packets. The first effort, in this direction, will take place this spring as driven by an undergrad research assistant.

Personnel

The early stages of this grant supported the final stages of the PhD of Qi Zhou. Dr. Zhou then spent 2 years at U. of Cambridge, U.K., as a postdoctoral researcher in the Department of Applied Mathematics and Theoretical Physics. As of Fall 2017, he has been an Assistant Professor in the Department of Civil Engineering at the U. of Calgary, Canada. The bulk of the funds in this grant supported postdoctoral researcher Kristopher Rowe, who worked on the analysis of internal wave energetics and drove the majority of the code redevelopment effort. As of September 2019, Dr. Rowe assumed a position as an Applications Performance Engineer at the Argonne National Laboratories.

Publications generated by this project

Zhou, Q. (2015) "Far-Field Evolution of Turbulence-Emitted Internal Waves and Reynolds Number Effects on a Localized Stratified Turbulent Flow", *PhD thesis*, Cornell University.

Zhou, Q. and P.J. Diamessis "Lagrangian flows within reflecting internal gravity waves at a free-slip surface", *Physics of Fluids* , 27, 2015, Article 126601.

Watanabe T., Riley J.J., de Bruyn Kops, S.M. and Diamessis, P.J. and Zhou, Q., "Turbulent/nonturbulent interfaces in wakes in stably-stratified fluids", *Journal of Fluid Mechanics*, 797, 2016, R1.

Zhou, Q. and P.J. Diamessis "Surface manifestation of internal waves emitted by submerged localized stratified turbulence", *Journal of Fluid Mechanics*, 798, 2016, pg. 505-539.

Zhou, Q. and P.J. Diamessis, "Large-scale characteristics of stratified wake turbulence at varying Reynolds number", *Physical Review Fluids*, 4 (8), 2019, Article Number: 084802.

Rowe, K.L., P.J. Diamessis and Q. Zhou, "Internal gravity wave radiation from a stratified turbulent wake", (Accepted by *Journal of Fluid Mechanics*, 2019).

Awards linked to this project

Department of Defense High Performance Computing (HPC) Modernization Program,
2016 HPC Success Story Award for Project "Multiscale Interactions in Stratified Turbulence" ;
Collaborators and co-awardees for Project: Stephen M. de Bruyn Kops (P.I. ; U. Mass., Amherst), James J. Riley (U. Washington), Tomoaki Watanabe (U. Nagoya, Japan), Qi Zhou (Cambridge U.).